EARTHQUAKE ENGINEERING AND STRUCTURAL DYNAMICS
Earthquake Engng. Struct. Dyn. **28**, 1427–1447 (1999)

ACTUAL SEISMIC RESPONSE CONTROLLED BUILDING WITH SEMI-ACTIVE DAMPER SYSTEM

NARITO KURATA[1]*, TAKUJI KOBORI[2], MOTOICHI TAKAHASHI[1], NAOKI NIWA[1] AND HIROSHI MIDORIKAWA[3]

[1] *Kobori Research Complex, Kajima Corporation, KI Building, 6-5-30, Akasaka, Minato-ku, Tokyo 107-8502, Japan*
[2] *Professor Emeritus of Kyoto University, Dr. of Eng. and Chief Executive Adviser, Kajima Corporation, KI Building, 6-5-30, Akasaka, Minato-ku, Tokyo 107-8502, Japan*
[3] *Kajima Technical Research Institute, Kajima Corporation, KI Building, 6-5-30, Akasaka, Minato-ku, Tokyo 107-8502, Japan*

SUMMARY

This paper presents the first application of a semi-active damper system to an actual building. The Semi-active Hydraulic Damper (SHD) can produce a maximum damping force of 1000 kN with an electric power of 70 W. It is compact, so a large number of them can be installed in a single building. It is thus possible to control the building's response during a severe earthquake, because a large control force is obtained in comparison with a conventional active control system.

This paper outlines the building, the control system configuration, the SHD, the control method using a Linear Quadratic Regulator, the response analysis results of the controlled building, and the dynamic loading test results of the actual SHD. The simulation analysis shows that damage to building can be prevented in a severe earthquake by SHD control. The dynamic loading test results of the SHD are reported, which show that the specified design values were obtained in the basic characteristic test. The control performance test using simulated response time histories, also shows that the damping force agrees well with the command. Finally, it is confirmed that the semi-active damper system applied to an actual building effectively controls its response in severe earthquakes. Copyright © 1999 John Wiley & Sons Ltd.

KEY WORDS: structural control; semi-active control; semi-active hydraulic damper; linear quadratic regulator; velocity feedback; seismic response

1. INTRODUCTION

A semi-active control system can produce a large control force simply by dynamically changing parameters such as control device damping coefficient and stiffness. Therefore, it has the advantage that it can control the response of a large-scale structure in a severe earthquake with smaller energy in comparison with a conventional active control system utilizing an actuator. From this viewpoint, in 1991 the authors proposed the application to a building structure of a semi-active control system (Active Variable Damping system) utilizing variable damping element.[1] Similarly, in 1990 Kobori *et al.*[2] developed an on–off semi-active hydraulic damper and installed it in an actual three-storey building. Other proposals included those of Feng and Shinozuka[3] and Kawashima,[4] who proposed the application of a semi-active control system to

* Correspondence to: Narito Kurata, Senior Research Engineer, Kobori Research Complex, Kajima Corporation, KI Building, 6-5-30, Akasaka, Minato-ku, Tokyo 107-8502, Japan. E-mail: kurata@krc.kajima.co.jp

CCC 0098–8847/99/111427–21$17·50

Received 28 April 1999
Accepted 18 June 1999

a bridge. A lot of research and development of semi-active dampers has been carried out during the past several years because of their high performance and low power demand.

Semi-active device mechanisms are classified into three kinds. The first is a hydraulic damper with a controllable valve. It has achieved the best results, and can easily produce a large force. Kurata *et al.* have demonstrated the effectiveness of this semi-active control system through a control experiment on a large three-storey model structure using a shaking table,[5] and a simulation analysis of a semi-actively controlled high-rise building in severe earthquakes.[6] Mizuno *et al.*[7] and Kawashima[4] reported a performance test on a semi-active hydraulic damper with a maximum damping force of 200 kN. Symans and Constantinou reported shaking table experiments on a three-storey test structure.[8] Patten *et al.* developed a small size damper, carried out a detailed simulation of its performance[9] and applied it to an actual bridge.[10] The second type of the semi-active device is a controllable friction damper. Akbay and Aklan[11] proposed a friction slip brace. Dowdell and Cherry[12] proposed a variable slip force friction damper and an 'Off–On' friction damper. The performance of this system was compared with that of a constant slip force friction damper and a fully active tendon. Feng *et al.*[13] and Yang[14] investigated a friction-controllable sliding bearing. Hirai[15] investigated a variable friction damper utilizing piezoelectric actuators that change the load on a brake-pad. The third type of device is a controllable fluid damper. This device is mechanically reliable, because it contains no moving parts. Performance tests and modelings of the ER damper were carried out by Ehrgott and Masri,[16] Gavin *et al.*,[17] Makris.[18] Spencer Jr. *et al.*[19] and Carlson and Spencer Jr.[20] showed the characteristics of MR fluid as applied to semi-active control. In the above research, a Linear Quadratic Regulator (LQR) was applied most frequently as the control theory.[5,6,8,12,15] The maximum force of the device was in the order of tens of tons.

This paper presents the first application of a semi-active damper system to an actual building. It outlines the building, the control system configuration, the semi-active hydraulic damper (SHD) and the control method using LQR. The response analysis of the semi-actively controlled building in a severe earthquake was carried out to confirm the response reduction effect of this system. Furthermore, a dynamic loading test of an actual SHD with a maximum damping force of 1000 kN was carried out to confirm the basic characteristics and control performance using simulated response time histories.

2. OUTLINE OF BUILDING WITH SEMI-ACTIVE DAMPER SYSTEM

The semi-active damper system was applied to an office building comprising five stories and a basement located in Shizuoka City, Japan. A typical floor plan and a framework elevation of the building are shown in Figure 1(a) and (b), respectively. The building height is 19·75 m, the total floor area is 1685·36 m^2 and the total mass is 1 102 300 kg. It was designed in accordance with the Japanese seismic resistance design standards as a steel frame structure. The eight SHDs were installed in combination with steel braces on each storey from the first to the fourth on both gable ends in the short side direction. The seismic response of the building was expected to be reduced by this system and the structural safety during a severe earthquake was thus expected to be improved. Incidentally, elastoplastic steel dampers were installed in the long side direction. The configuration of the SHD system is shown in Figure 1(c). This system consists of velocity sensors on each floor, computers in the control room on the first floor, SHDs and an uninterruptible power supply unit. The control procedure was as follows: (i) the sensors measure the building

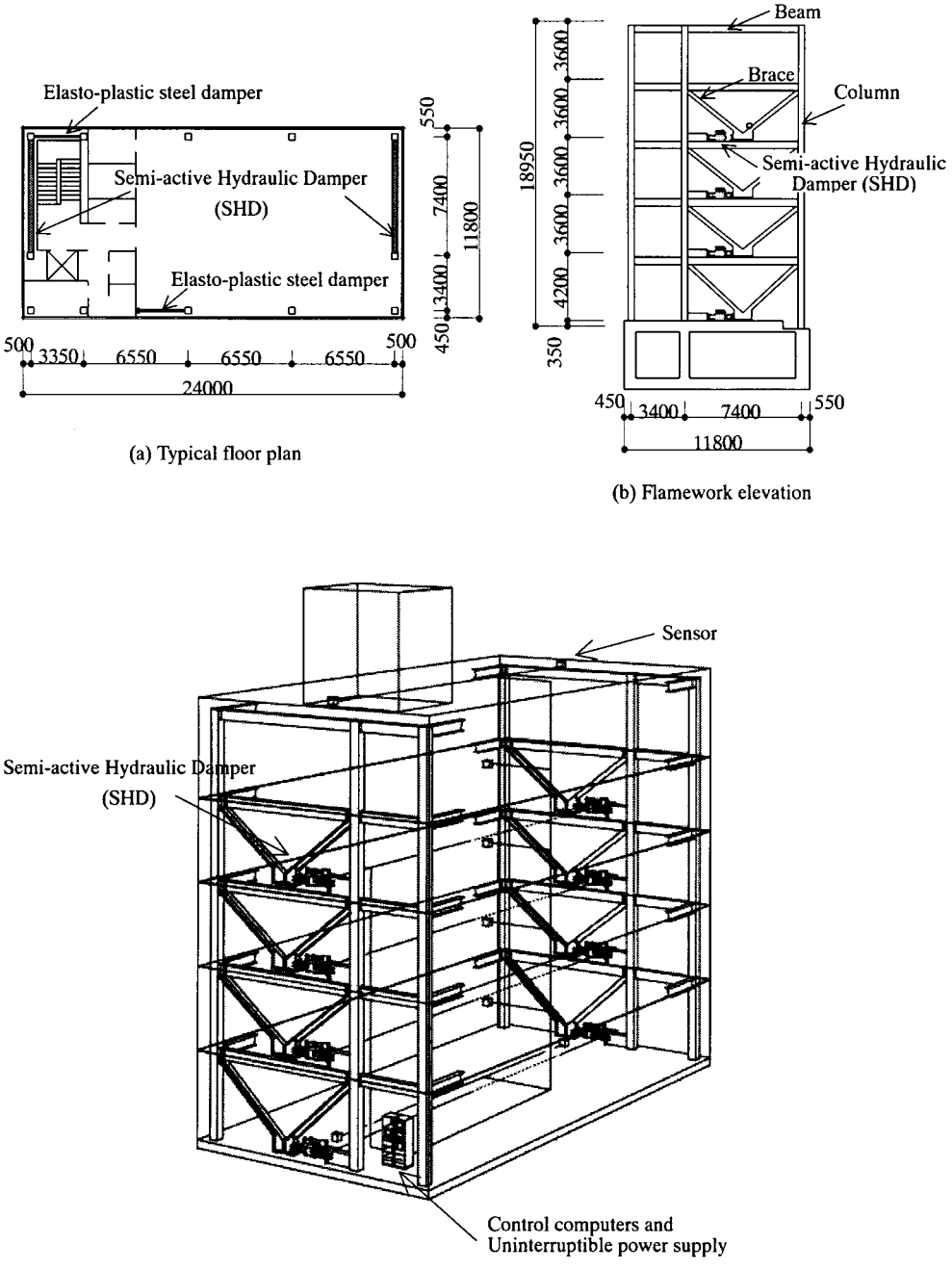

Figure 1. Building outline with SHD

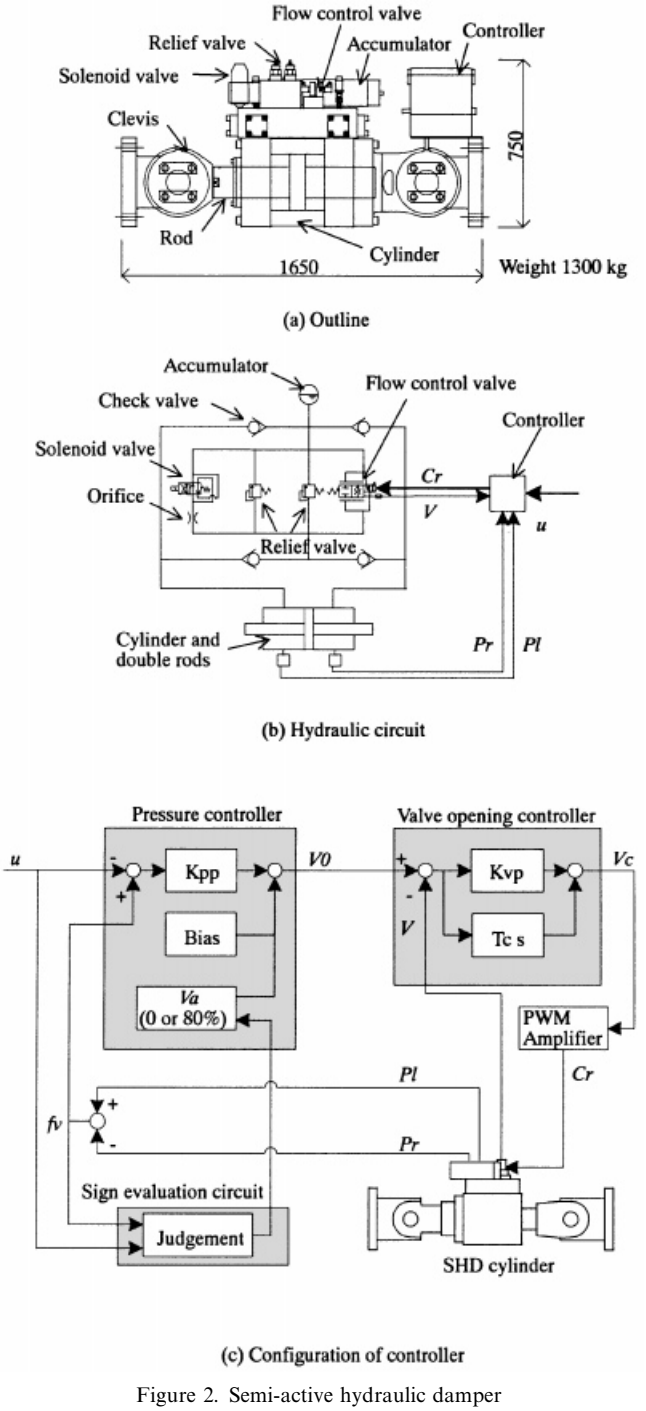

Figure 2. Semi-active hydraulic damper

responses; (ii) the computers calculate the damping force command to minimize the response based on the detected data; and (iii) SHDs generate the damping forces according to the computer command. Even in case of a power failure, the system can still function with the uninterruptible power supply unit.

3. CONFIGURATION OF SEMI-ACTIVE HYDRAULIC DAMPER (SHD)

A full-size SHD with a maximum damping force of 1000 kN has been developed. Its outline and specifications are shown in Figure 2(a) and Table I, respectively. It consists of a cylinder, double rods and a manifold in which several hydraulic units are installed, and is connected by bolts to a brace and a bracket fixed at the column end through clevises on both sides. Clevises can revolve in any rotating direction and eliminate the external force in the other direction of the cylindrical axis. It is compact and a special establishment place is unnecessary, so a large number of them can be installed in a building. Figure 2(b) shows the hydraulic circuit of the SHD. It comprises a flow control valve, a check valve and an accumulator. The SHD controller regulates the damping force f_v by simply adjusting the opening rate V of the flow control valve between the cylinder chambers. Because the flow control valve is composed two stages, a main spool and a pilot spool, it requires an electric power of only about 70 W. The check valves ensure that the oil flow in the hydraulic circuit moves in only one direction through the flow control valve. An accumulator is provided to supply oil to compensate for the volume loss due to compression. The relief valve that opens with a set pressure is installed in parallel to the flow control valve, so that the load cannot cause the design stress of the SHD exceed. Furthermore, a solenoid valve that opens in the case of interruption of the electrical service is provided as a fail-safe to an unexpected system fault or power failure. When it opens, the oil flows through the orifice and the SHD works as a passive damper. The SHD controller, shown in Figure 2(c), consists of a pressure controller, a valve opening controller and a sign evaluation circuit. The pressure controller converts the damping force command u to a valve opening command V_0 to minimize the deviation between the actual damping force f_v and damping force command u using the feedback hydraulic pressure P_l and P_r, the inside left and right parts of the cylinder. The valve opening controller distributes control current C_r to the flow control valve to minimize the deviation between the actual valve opening V and valve opening command V_0 from the pressure controller. The SHD can produce a damping force f_v in the same direction as its velocity. If the direction of the damping force command u and

Table I. Specification of SHD

Maximum damping force	1000 kN
Relief load	800–900 kN
Maximum pressure	30 MP
Maximum displacement	$\pm$ 60 mm
Stiffness (including bracket)	$>$ 400 kN/mm
Maximum damping coefficient	$>$ 200 kN sec/mm
Minimum damping coefficient	$<$ 1 kN sec/mm
Maximum velocity	250 mm/sec
Diameter	390 mm
Weight	1300 kg

the actual damping force f_v are not the same, the sign evaluation circuit introduces an additional valve opening command V_a not to generate a damping force. The controller parameters K_{pp}, K_{vp}, Bias and T_c are the proportional gains of the pressure controller and the valve opening controller, the bias value and the differential time constant, respectively. They are decided on the basis of the test results described in Section 5 to optimize the following performance of the actual damping force to command.

4. ANALYTICAL VERIFICATION OF CONTROL EFFECT

The aim of research and development of the semi-active damper system is to secure the structural safety and functionability of buildings during severe earthquakes, and to improve even uncomfortable vibration caused by small earthquakes. This section describes the simulation analysis of a building with semi-active control to confirm the system's control performance.

4.1. Analytical model

The analytical model for the short side direction of the building with the semi-active damper system was analysed. The building was modelled as a lumped mass system in which the weight of each storey is concentrated at each floor level and the columns and beams are represented by equivalent shear springs. Details of the analytical model are shown in Table II. The inherent damping of the building was assumed to be 2 per cent for the internal damping ratio to the first natural period. The primary third natural periods of the building without SHDs are 0·992, 0·354 and 0·222 sec.

The SHD was installed between the bracing and the beam in the structural plane, as shown in Figure 3(a). A model of the SHD and bracing are shown in Figure 3(b). The SHD is expressed by the combination of stiffness element Kd and a variable damping element with a damping coefficient $c(t)$ in series. Furthermore, an element comprising Kb and SHD were incorporated into the building model. The stiffness Kd of the SHD in Figure 3 is an important physical quantity that greatly influences the performance of the control system. As series stiffness Kd and Kb are bigger than frame stiffness Kf, the deformation is dominated by the variable damping element $c(t)$ and a high response reduction effect is obtained. The upper limit value of the damping force f_{max} and the maximum damping coefficient c_{max} for every SHD were set a 900 kN, which was the relief load, and 200 kN sec/mm, respectively.

Table II. Details of analytical model

Floor	Mass	Stiffness		
	(kg)	Frame Kf (kN/mm)	Brace Kb (kN/mm)	SHD Kd (kN/mm)
5	266 100	84	—	—
4	204 800	89	565 × 2	
3	207 000	99	565 × 2	400 × 2
2	209 200	113	565 × 2	
1	215 200	147	438 × 2	

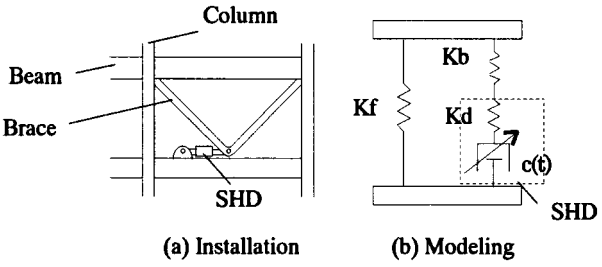

Figure 3. Installation and modelling of semi-active hydraulic damper

4.2. *Input earthquake motions*

El Centro (1940 NS), Taft (1952 NS) and Hachinohe (1968 NS) were adopted as the input earthquake motions. The assumed Tokai artificial earthquake motion which had a maximum acceleration of 3·29 m/sec^2 and a maximum velocity of 0·71 m/sec was also used. It was evaluated on the basis of a fault parameter of the Ansei Tokai earthquake with magnitude 8·4 in 1854, the severest to occur in the Tokai district.[21,22] The acceleration response spectra for El Centro, Taft and Hachinohe waves with scaled maximum velocity of 50 cm/sec, and assumed Tokai wave, are shown in Figure 4.

4.3. *Control system design*

The SHD produces a damping force in accordance with the command from the computer. The damping force f_{vi} of the ith SHD is expressed by the following equation.

$$f_{v_i} = \begin{cases} f_{\max} \times \operatorname{sign}(v_i) & u_i \times v_i > 0,\ |u_i| > f_{\max} \\ c_{\max} \times v_i & u_i \times v_i > 0,\ |u_i/v_i| > c_{\max},\ |u_i| \leqslant f_{\max} \\ c_i(t) \times v_i = u_i & u_i \times v_i > 0,\ |u_i/v_i| \leqslant c_{\max},\ |u_i| \leqslant f_{\max} \\ 0 & u_i \times v_i \leqslant 0 \end{cases} \tag{1}$$

where u_i is the damping force command from the computer to the ith SHD and v_i is the ith SHDs velocity. $f_{\max}$ and $c_{\max}$ are the upper limit value of the damping force and the maximum damping coefficient of the SHD, respectively.

The damping force command to the SHD is designed to minimize the building's response, and various control theories can be applied to the calculation. The relative velocity feedback law based on Linear Quadratic Regulator (LQR) is adopted. The physical meaning of this control law is evident and it is easy to design a MIMO control system. The formulation of the LQR is as follows. The state equation is

$$\dot{X}(t) = AX(t) + BU(t) + DW(t) \tag{2}$$

where $X = \{x\ \dot{x}\}^{\mathrm{T}}$ is the state-space vector, U the control force vector, and W the disturbance vector.

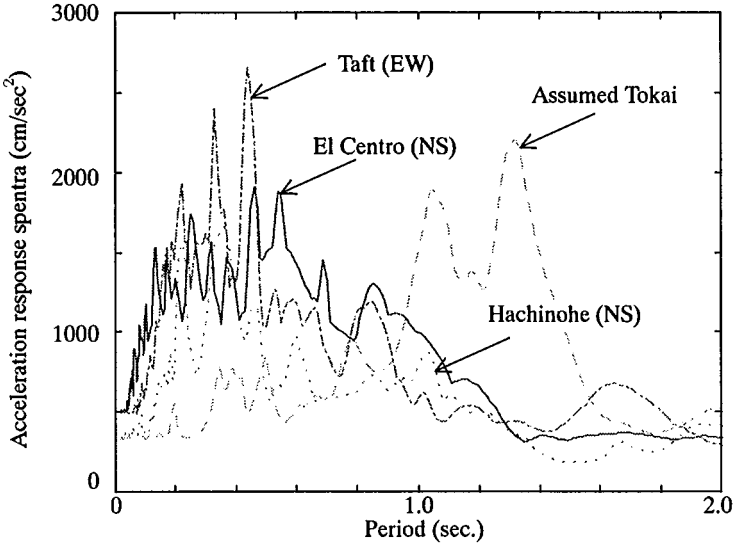

Figure 4. Acceleration response spectra of input earthquake motions (damping ratio $h = 0{\cdot}02$)

The performance index is

$$J = \int_0^\infty [X(t)^{\mathrm{T}} QX(t) + U(t)^{\mathrm{T}} RU(t)]\,\mathrm{d}t \tag{3}$$

where Q and R are weighting matrices.

The optimal control force without consideration of the disturbance is

$$U(t) = -R^{-1} B^{\mathrm{T}} PX(t) = -GX(t), \quad G = [[G_{\mathrm{d}}][G_{\mathrm{v}}]] \tag{4}$$

where $[G_{\mathrm{d}}]$ and $[G_{\mathrm{v}}]$ are the feedback gain sub-matrix with respect to the displacement and velocity, respectively. P is the solution of the following Ricatti equation:

$$PA + A^{\mathrm{T}} P + Q - PBR^{-1} B^{\mathrm{T}} P = 0 \tag{5}$$

LQR was applied to the building model described in Section 4.1. The weighting parameters in equation (3) are given in the following equation:

$$Q = \begin{bmatrix} [Q_{\mathrm{v}}] & [0] \\ [0] & [Q_{\mathrm{d}}] \end{bmatrix}, \quad [Q_{\mathrm{v}}] = \mathrm{diag}\ (1), \quad [Q_{\mathrm{d}}] = O, \quad R = \mathrm{diag}(r) \tag{6}$$

To determine the control gain, 13 kinds of feedback gain were calculated for the building model by changing r to 1–0·01. The obtained gain is the full matrix with respect to both the displacement and velocity. However, since the gain with respect to the displacement is negligible, velocity feedback control is adopted, i.e., $[G_{\mathrm{d}}] = O$.

Substituting equation (4) into equation (2), the state equation can be expressed as

$$\dot{X}(t) = (A - BG)X(t) + DW(t) \tag{7}$$

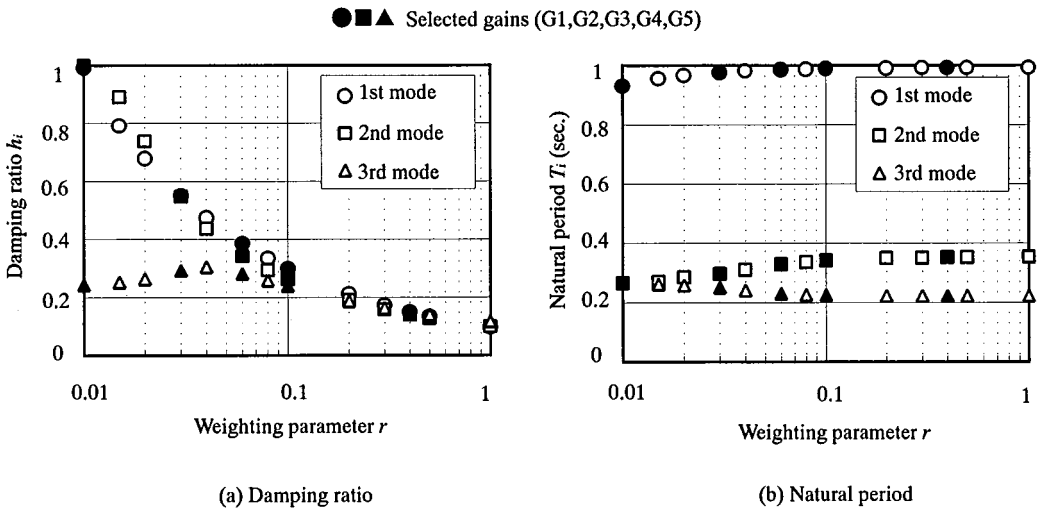

Figure 5. Damping ratio and natural period of actively controlled building model

The damping ratio h_i and natural period T_i of the actively controlled building model to the ith mode obtained by the eigenvalue of $(A - BG)$ in the above equation are shown in Figure 5. As r becomes small, h_1 and h_2 increase monotonously and T_i is almost constant. Because the SHD is not installed in the 5th storey, the trend of h_3 is different from those of h_1 and h_2. The five gains shown in black in this figure were selected. G1, G2, G3, G4 and G5 correspond to $r = 0{\cdot}4$, $0{\cdot}1$, $0{\cdot}06$, $0{\cdot}03$ and $0{\cdot}01$. The feedback gain by LQR for the discrete-time system corresponding to a digital computer in this system is used in the seismic response analyses in Section 4.4. The sampling time was assumed as $0{\cdot}005$ sec.

4.4. Seismic response analysis

A seismic response analysis of the building model described in Section 4.1 was carried out using the feedback gain selected in Section 4.3. The El Centro wave with its maximum velocity normalized to 10, 25 and 50 cm/sec was used as the input motion. Figure 6 shows the maximum values of top acceleration, base shear force and storey drift in all stories, divided by the maximum velocity of the input motion. The base shear force of the building without control (indicated as NC) exceeded the elastic limit for the El Centro wave with its maximum velocity scaled to 25 and 50 cm/sec. Thus, the elastoplastic response with additional hysteretic damping becomes relatively small as input velocity becomes large. However, all of the controlled responses are in the elastic range and the damping force of the SHD on the 1st floor reaches its upper limit in the cases of G5 for the 25 cm/sec input and G2, G3, G4 and G5 for the 50 cm/sec input. However, the responses divided by the input velocity at each gain are almost the same and the control performance is not degraded in spite of the limitation of the damping force. Generally, the damping force increases and the response decreases with increase in gain number. Whether or not the damping force reaches its upper limit, the acceleration and storey drift becomes minimum at G2 and G3, respectively. The large gain should be used to reduce the shear force, because it becomes a minimum at G5 for 10 and 25 cm/sec input.

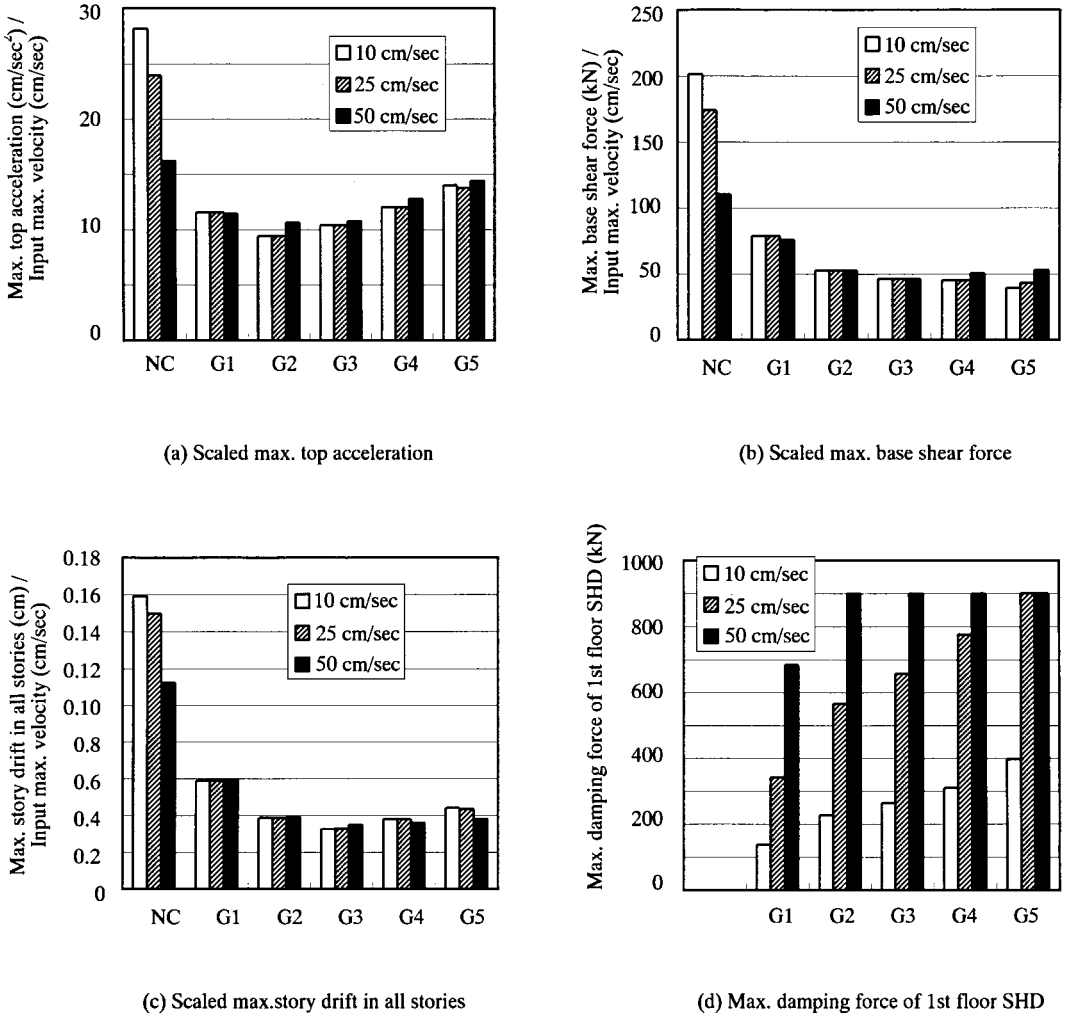

Figure 6. Effect of amplitude of input earthquake motion (El Centro 10, 25 and 50 cm/sec)

The simulation analyses for the El Centro, Taft and Hachinohe waves with the scaled maximum velocity of 50 cm/sec, and the assumed Tokai wave, were carried out to confirm the control performance of this system under severe earthquakes. Figure 7 shows the resulting maximum responses. Reflecting the amplitude of response spectra around the first mode of the building shown in Figure 4, the uncontrolled response for the assumed Tokai is largest and that for Hachinohe is smallest. Although the general trend of the responses vs. gains is common with each wave, the maximum base shear force and the maximum storey drift in all stories reduce monotonously within the range of these gains for the assumed Tokai and Hachinohe waves. The top acceleration, base shear force and storey drift, when control by G4 is implemented, are reduced to 58–79, 38–59 and 25–43 per cent, respectively, of the values without control.

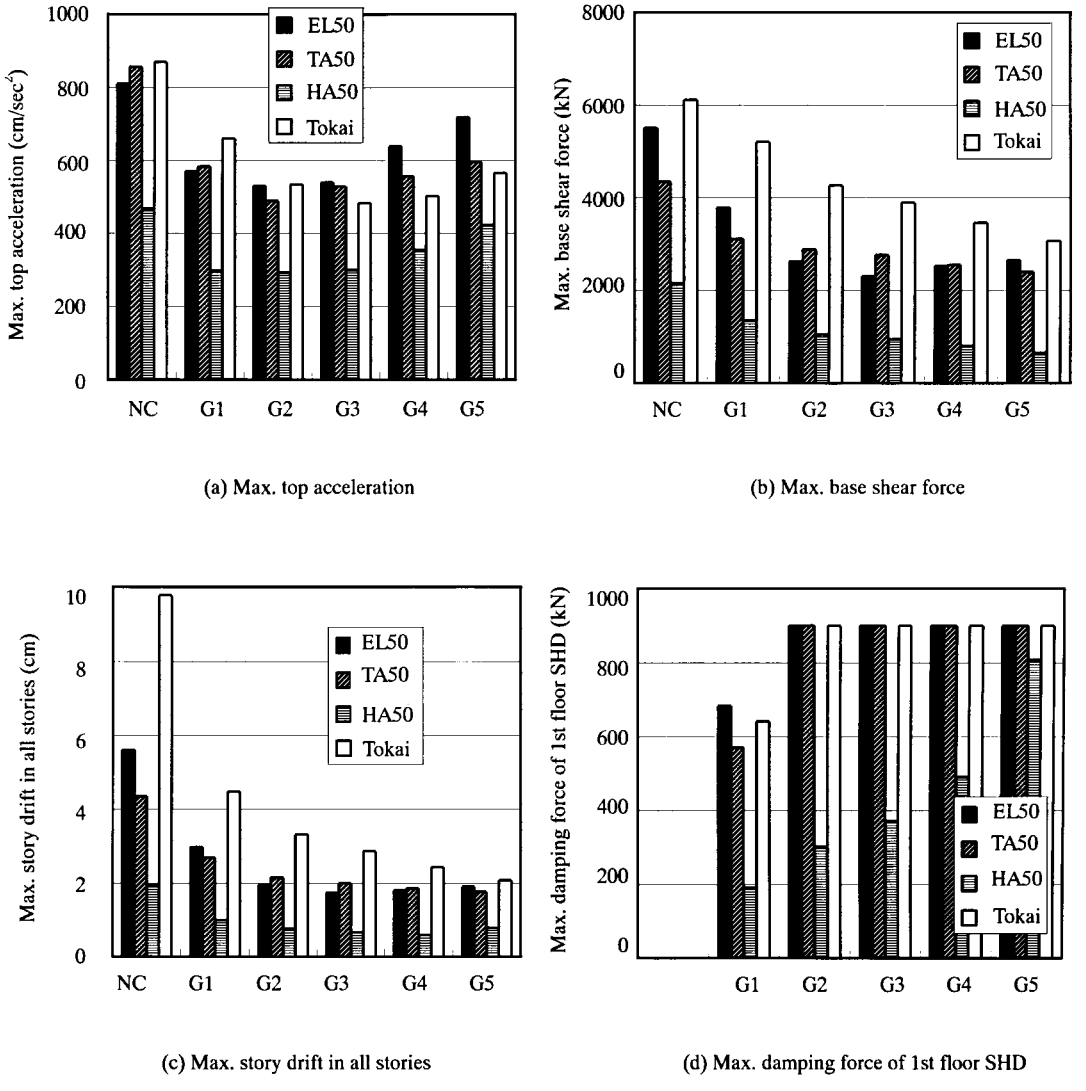

Figure 7. Control performance for large earthquakes (El Centro, Taft and Hachinohe waves with 50 cm/sec and assumed Tokai waves)

The maximum response distributions for the cases with SHD control by G4 and without control are shown in Figure 8. The shear force without control enters the plastic range, exceeding the elastic shear force. However, the shear force with SHD control is greatly reduced to within or around the elastic limit shear force (indicated as E-limit). This shows that the building frame would not be damaged even in severe earthquakes. It was thus proved that this semi-active damper system improved the structural safety of the building. Without control under the assumed Tokai wave, the storey drift exceeded 10 cm. With SHD control, by contrast, the storey drift angle was approximately 1/200 under all of the earthquakes, which was the deformation range in which the various building functions will be maintained.

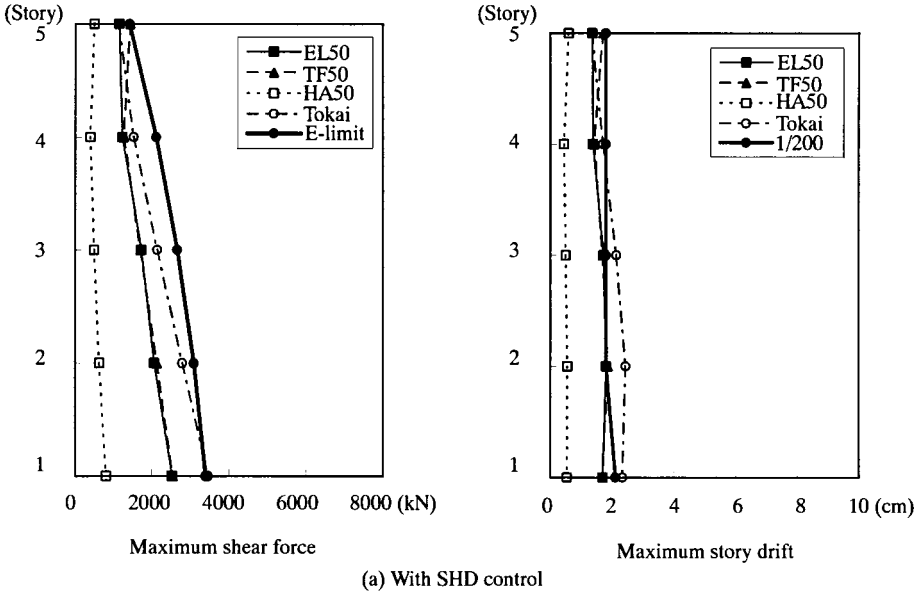

(a) With SHD control

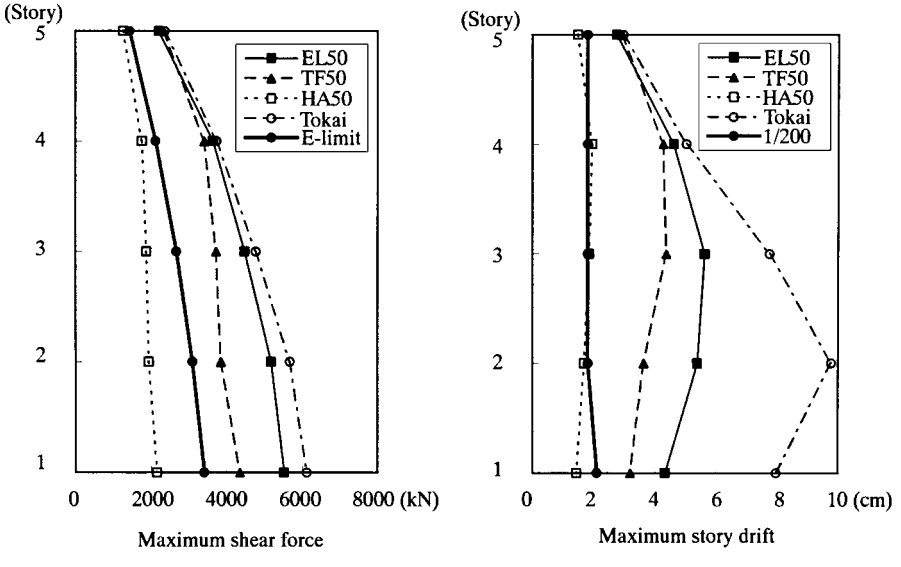

(b) Without control

Figure 8. Maximum responses (El Centro, Taft and Hachinohe waves with 50 cm/sec and assumed Tokai waves)

5. PERFORMANCE TEST OF SHD

5.1. Test method

A dynamic loading test was carried out to determine the basic characteristics and the control performance of the SHD. It is verified whether the design specification of the SHD shown in Table I is realized. The control performance test confirms the traceability of the actual damping force to the damping force command when the SHDs are installed in the building and subjected to an earthquake. Figure 9 shows the composition of the test equipment. The SHD was connected to the two actuators with a maximum force of 1000 kN. The actuators were attached to sturdy loading frames by a sliding guide. The damping force command u to the SHD and the displacement command x to the actuators are sent to the SHD controller and the excitation system, respectively, from the computer.

5.2. Basic characteristic test

The dynamic loading test under the sinusoidal wave was carried out to confirm the basic characteristic of the SHD. Figure 10(a) and (b) show the damping force F–total displacement DT and damping force F–velocity V_d response when the flow control valve was fully closed. The exciting frequency was 1·0 Hz and actuator load $\pm$ 300 kN. V_d is the differentiated value of the displacement that subtracted the deformation of oil from the rod–cylinder displacement D of the SHD. DT is the total displacement of the SHD. The stiffness of the SHD evaluated by the linear approximation in Figure 10(a) is 422 kN/mm. The maximum damping coefficient evaluated from the general trend in Figure 10(b) is 2000 kN sec/mm. Figure 10(c) shows the F–D and F–V_d responses when the flow control valve is fully open. The exciting frequency and maximum D are 1·0 Hz and 32 mm, respectively. In this case, the small force is generated by the cracking pressure of each valve, the friction between the rod and the cylinder and small viscous damping of oil with

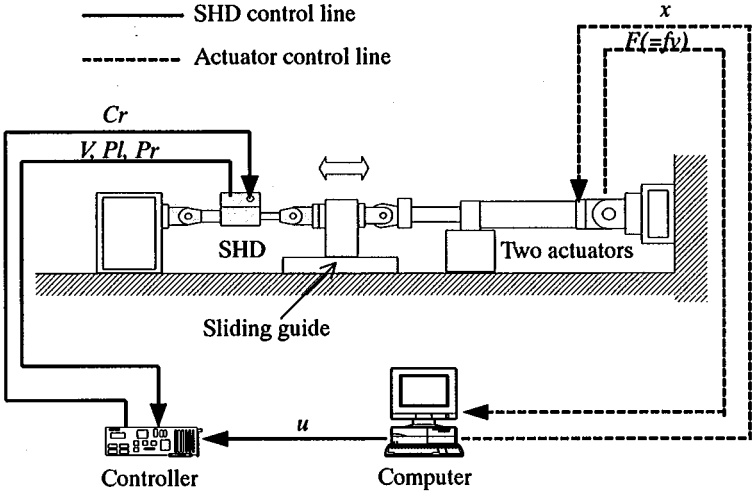

Figure 9. Composition of test equipment

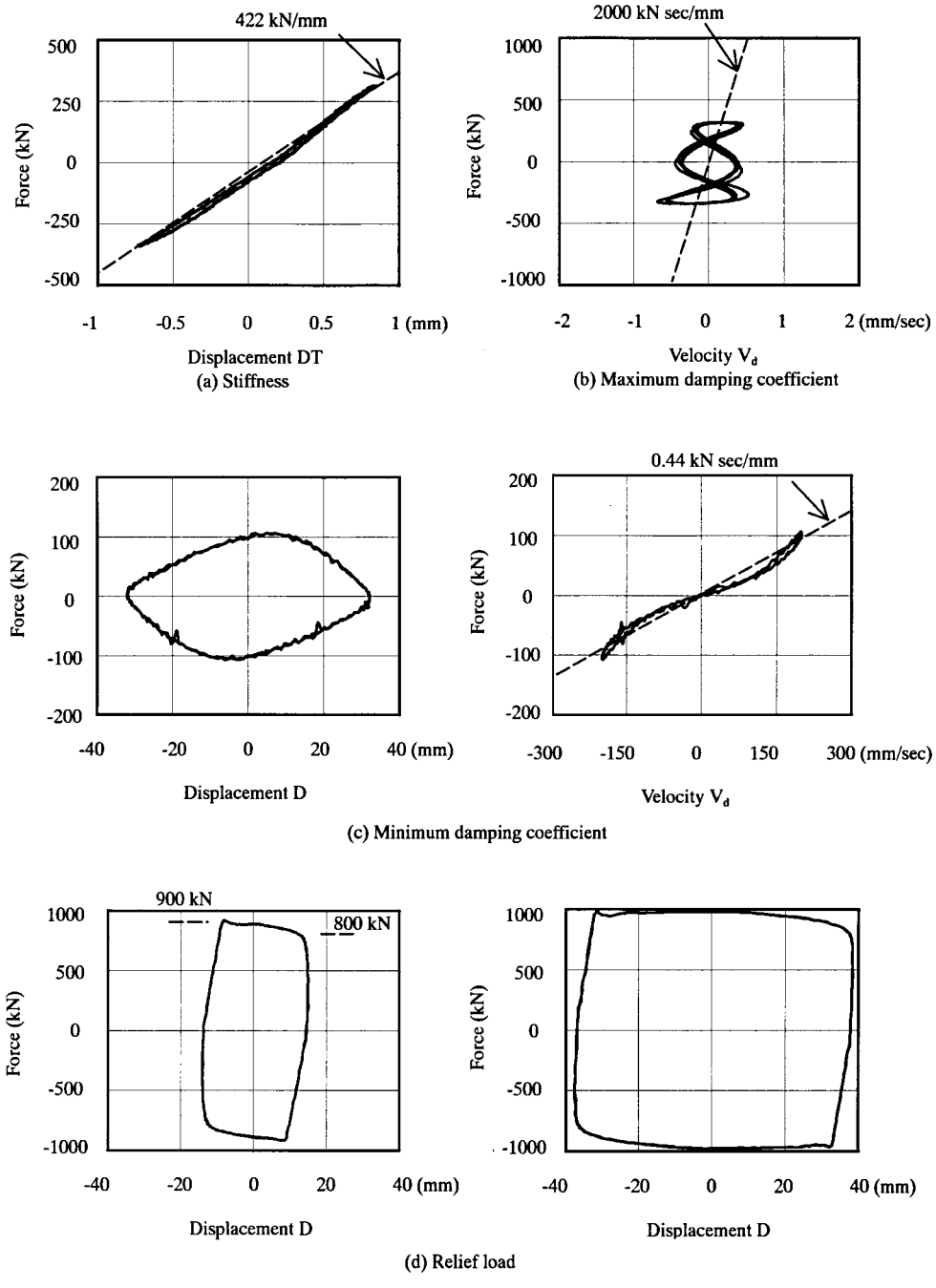

Figure 10. Force-displacement and force-velocity loops

a maximum velocity V_d of 20 cm/sec. The minimum damping coefficient evaluated from the linear approximation in Figure 10(c) is 0·44 kN sec/mm. Figure 10(d) shows the F–D response when the solenoid valve is open, the orifice and the relief valve are activated, and the flow control valve is fully closed. The excited frequency is 1·0 Hz and values of maximum D are 15 and 38 mm, respectively. The relief load is between 800 and 900 kN, and the damping force is not exceeded at $V_d = 24{\cdot}4$ cm/sec ($D = 38$ mm), which is almost equal to the design maximum velocity of 25 cm/sec. The test results satisfy the specification shown in Table I.

5.3. *Control performance test*

The dynamic loading test using the resulting time histories of simulation analysis described in Chapter 4 was carried out to confirm the control performance of the SHD. The test procedure is as follows: (i) the storey drift and the damping force command previously obtained in the simulation analysis of the controlled building were inputted to the computer; (ii) the command was transmitted to the SHD controller, which transformed the valve opening command to the flow control valve in the SHD; and (iii) the brace deformation x_b in the building calculated from the actuator load F was dynamically subtracted from the storey drift x_s. Evaluated displacement x was then outputted to the actuators as the displacement to be induced to the SHD.

$$x(n+1) = x_s(n+1) - x_b(n+1), \quad x_b(n+1) = K_1 x_b(n) + K_2 F(n)$$
$$K_1 = \exp[-K_b \Delta t / C_b],\ K_2 = (1 - K_1)/K_b \tag{8}$$

where K_b and C_b are the stiffness and damping coefficient of braces. With this procedure, it is possible to evaluate the control performance of the SHD when it is installed in the building.

The controller gains were decided by trial and error to optimize the following performance of the actual damping force to the command. The analytical results of G4 for El Centro with a maximum velocity of 25 cm/sec discussed in Chapter 4 were used mainly to adjust the controller gains, as it is able to correspond widely from G2 to G5. The controller gains shown in Figure 2(c) are tuned as follows: $K_{pp} = 1{\cdot}9531$, $K_{vp} = 3{\cdot}125$, $T_c = 40$ msec. The variable bias was changed from 17 to 34 per cent in accordance with the amplitude of the actual damping force of the SHD (10–800 kN). The test results of G3, G4 and G5 discussed in Chapter 4 with the tuned controller gains for the El Centro wave with its maximum velocity scaled to 25 and 50 cm/sec, are shown in Figure 11. This figure compares the actual damping force and the command of the SHD installed on the first floor and the third floor. As the gain increases, the damping force increases and reaches its upper limit in the cases of G5 for 25 cm/sec input and G3, G4 and G5 for 50 cm/sec input. The relief valve was activated, and this restricted the damping force to 900 kN when an excessive command was given. The actual damping force followed the command well in cases of G3 and G4, regardless of the storey and the maximum velocity of the input motion. The slight deviation between the damping force and the command can be seen in case of G5.

The test results of G4 for the El Centro, Taft and Hachinohe waves with a scaled maximum velocity of 25 cm/sec, and the assumed Tokai wave, are shown in Figure 12. There is no difference in control performance for the four kinds of input motions. The actual damping force followed the command well, regardless of the amplitude of the damping force and frequency component of the input motions.

The results that changed the controller gains are shown in Figures 13 and 14, to determine the validity of the tuned controller gain. The test was carried out in cases of G4 for the El Centro

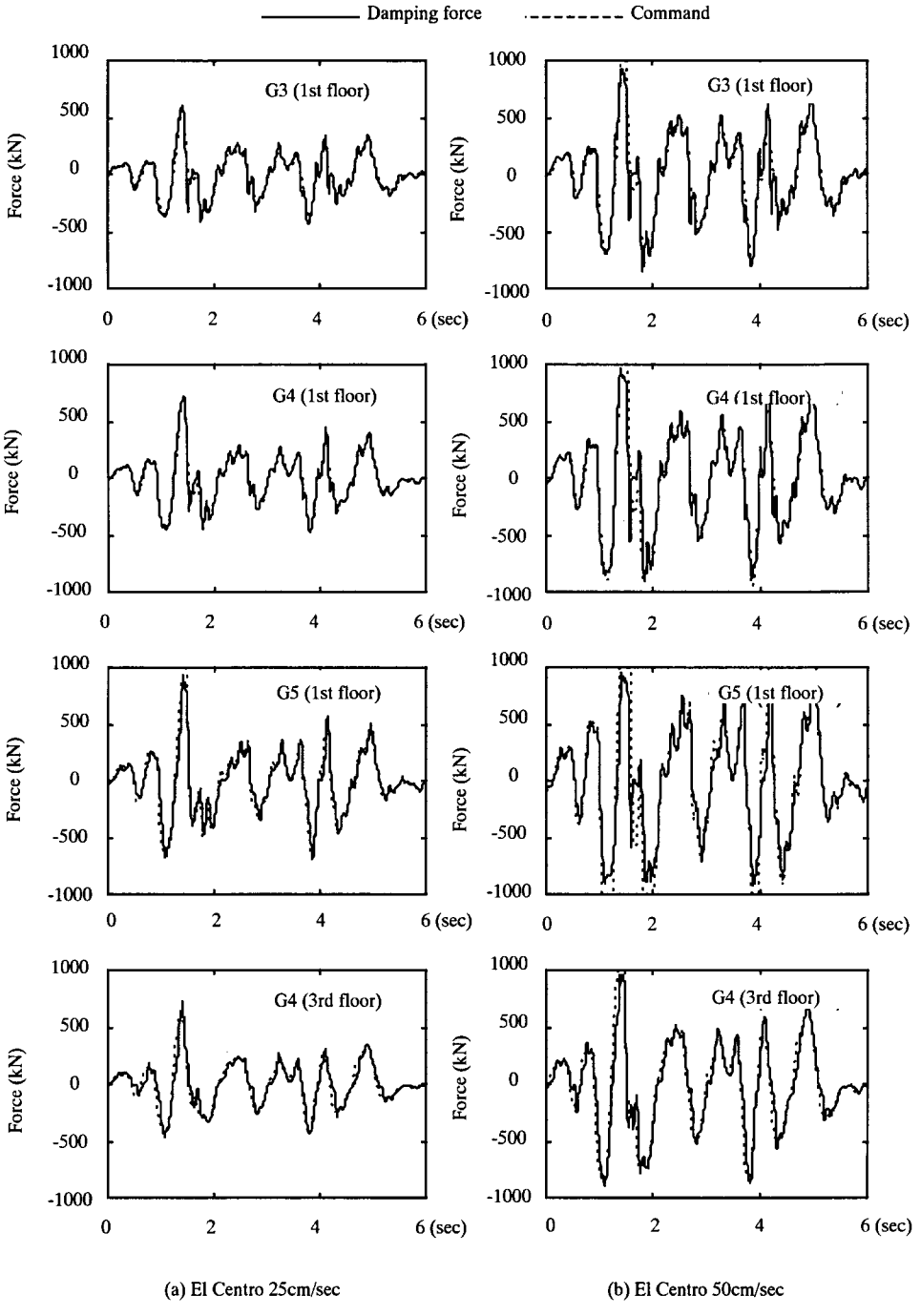

Figure 11. Effect of control gains and amplitude of input earthquake motion

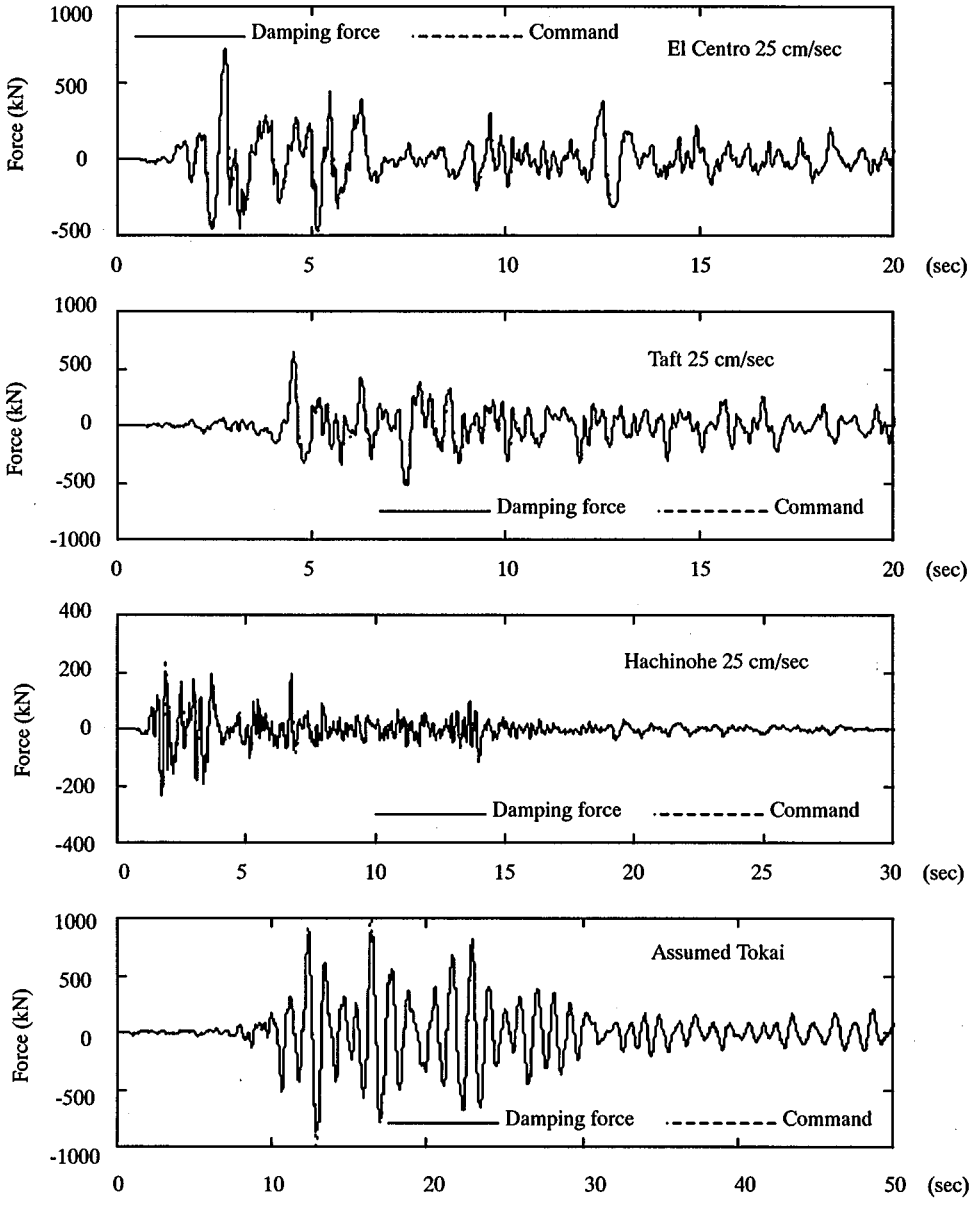

Figure 12. Effect of input earthquake motions (El Centro, Taft, Hachinohe and Assumed Tokai)

wave with its maximum velocity scaled to 25 cm/sec by changing only one gain of the combination of tuned gains. The comparative result of the cases where Bias was variable and fixed to the upper (34 per cent) or lower (17 per cent) bound value, is shown in Figure 13. Overshooting of the damping force is seen at the peak, because the valve opening rate is small for Bias = 17 per cent. However, the damping force followed the command very well in a small force area. The valve

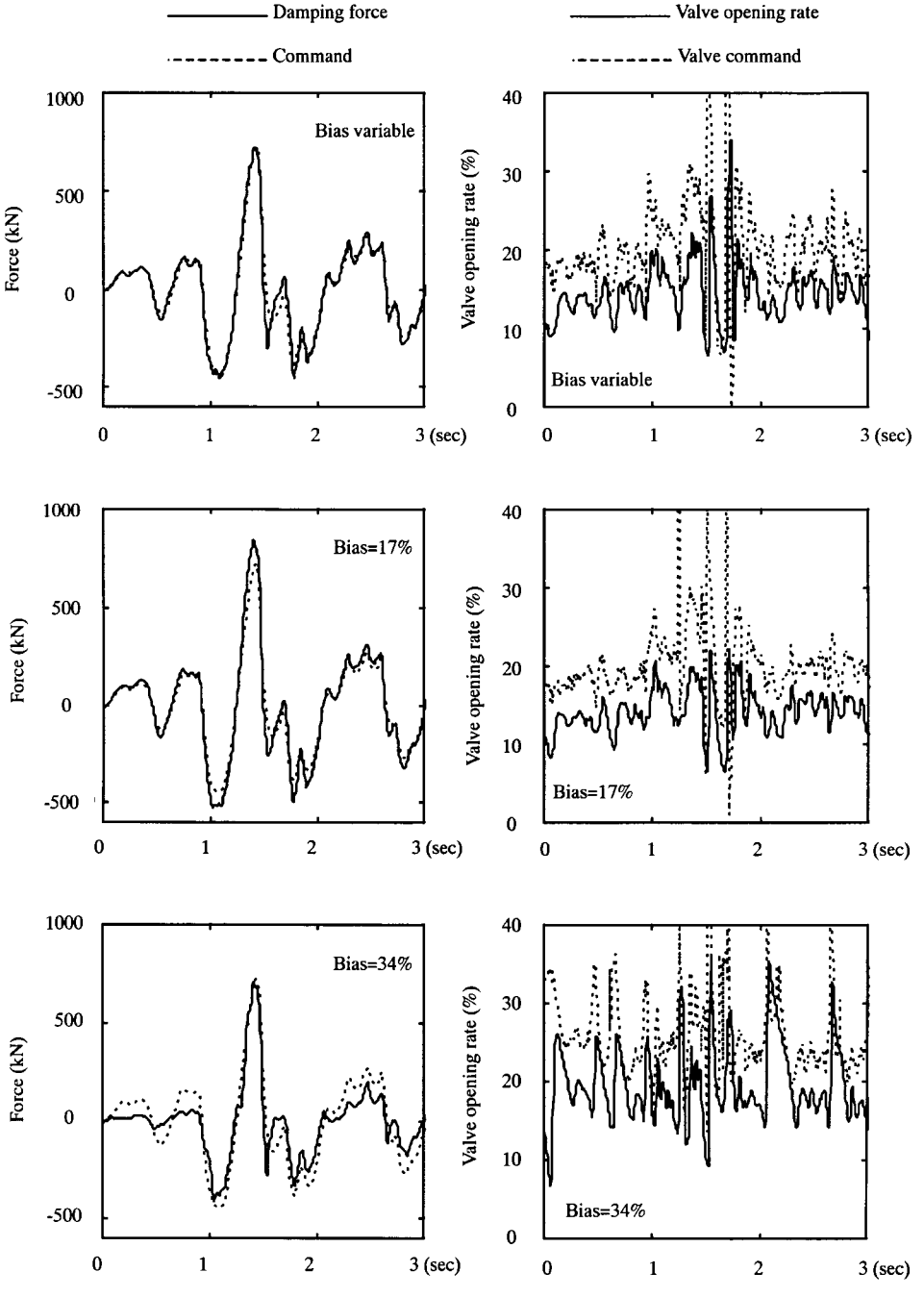

Figure 13. Effect of controller gains (El Centro 25 cm/sec)

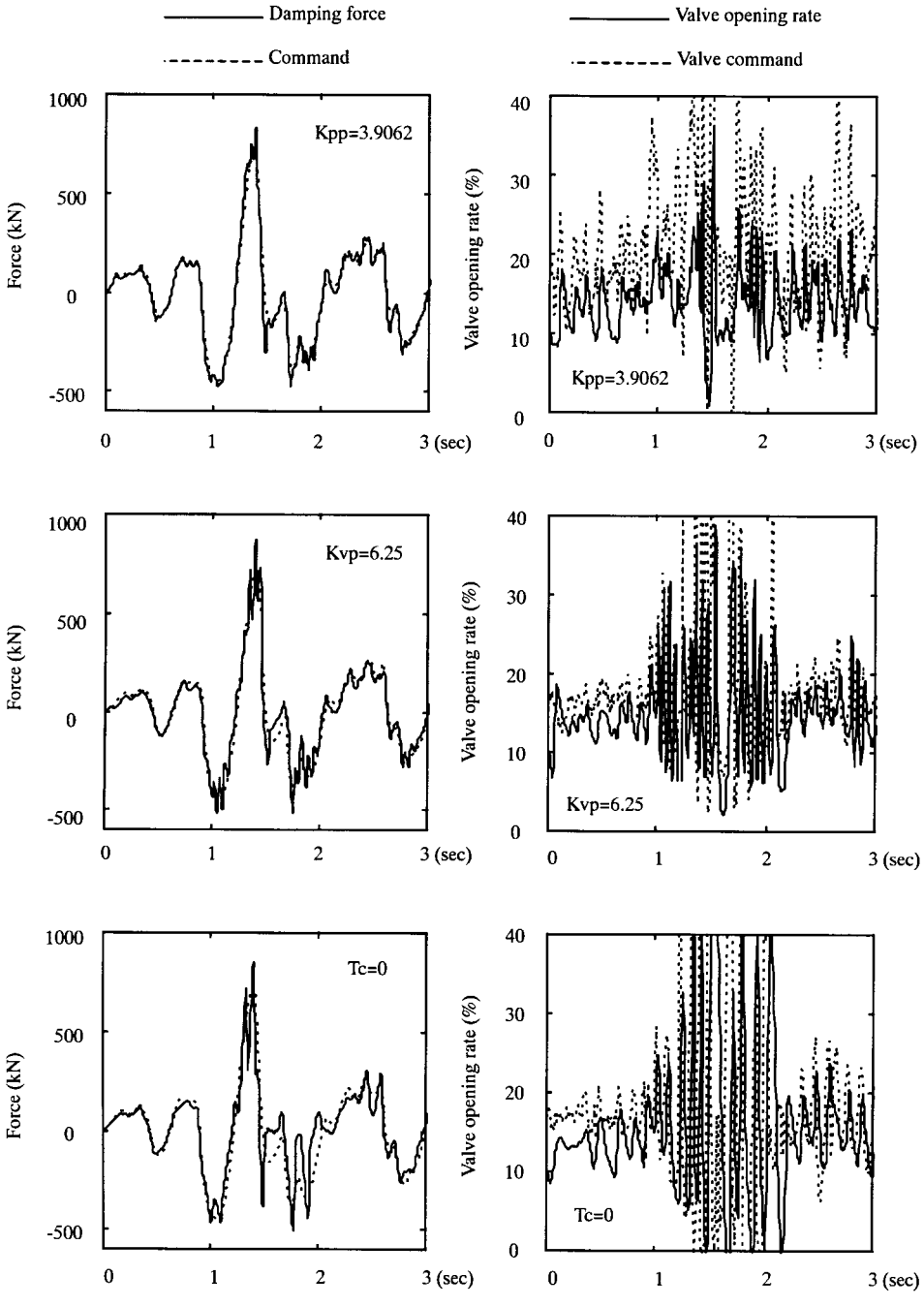

Figure 14. Effect of controller gains (El Centro 25 cm/sec)

opening rate is large in the case of Bias = 34 per cent, and the damping force is small over most of the range. The damping force at the peak produces an optimum amplitude without overshooting. Variable Bias prevents overshooting by opening the valve at the peak point, so that the damping force is caused to agree with the command by closing the valve in the small pressure area. The results in which K_{pp} and k_{vp} are doubled, $K_{pp} = 3{\cdot}9062$ and $K_{vp} = 6{\cdot}25$, and $T_c = 0$ without the differentiating circuit are shown in Figure 14. When K_{pp} and K_{vp} are large, the deviation of damping force command and damping force, or the deviation of valve opening rate command and actual valve opening rate, become small. However, the valve vibrates at a high frequency when K_{pp} and K_{vp} are too large. Furthermore, the valve was not able to follow the sharp change of the command and vibrated without the differentiating circuit ($T_c = 0$). The above results confirm the validity of the tuned controller gain.

6. CONCLUSIONS

The paper has presented the first application of a semi-active damper system to an actual building. This system controls a building's response in severe earthquakes with a small amount of electric power. The building and system configuration, and the structure of semi-active hydraulic damper (SHD) with the maximum damping force of 1000 kN, were outlined. The response control performance of the system was confirmed through a simulation analysis. Damage to the building can be avoided in a severe earthquake with this system. Results of a dynamic loading test using the SHD were also reported. The specified design values were obtained in the basic characteristic test. The damping force agreed closely with the command in the control performance test that used simulated response time histories. Finally, it was confirmed that the semi-active damper system applied in an actual building was effective in controlling the response of the building during a severe earthquake.

ACKNOWLEDGEMENTS

The authors would like to express their gratitude to Messrs. Y. Matsunaga and T. Mizuno of Kajima Corporation for developing the SHD and to the Kawasaki Heavy Industry Ltd. for manufacturing SHD.

REFERENCES

1. T. Kobori, M. Takahashi, N. Niwa and N. Kurata, 'Research on active seismic response control system with variable structure characteristics—feedback control with variable stiffness and damping mechanism', *J. Struct. Engng. AIJ* **37B**, 193–202 (1991).
2. T. Kobori, M. Takahashi, T. Nasu, N. Niwa and K. Ogasawara, 'Seismic response controlled structure with active variable stiffness system', *Earthquake Engng. Struct. Dyn.* **22**, 925–941 (1993).
3. Q. Feng and M. Shinozuka, 'Use of a variable damper for hybrid control of bridge response under earthquake', *Proc. U.S. Nat. Workshop on Struct. Control Res.*, USC Publ. No. CE-9013, 1990.
4. K. Kawashima, 'Experiments on dynamics characteristics of variable damper', *Proc. Japan Nat. Symp. on Struct. Resp. Cont.*, 1992, p. 121.
5. N. Kurata, T. Kobori, M. Takahashi, N. Niwa and H. Kurino, 'Shaking table experiment of active variable damping system', *Proc. 1st World Conf. on Structural Control*, 1994, Vol. 2, TP2, pp. 108–117.
6. N. Kurata, T. Kobori, M. Takahashi and N. Niwa, 'Active variable damping system in large earthquakes', *Proc. 3rd Int. Conf. on Motion and Vibrational Control,* 1996, Vol. 3, pp. 285–290.
7. T. Mizuno, T. Kobori, J. Hirai, Y. Matsunaga and N. Niwa, 'Development of adjustable hydraulic damper for seismic response control of large structure', *ASME PVP Conf.* 1992, Vol. 229, pp. 163–170.
8. M. D. Symans and M. C. Constantinou, 'Seismic testing of a building structure with a semi-active fluid damper control system', *Earthquake Engng. Struct. Dyn.* **26**, 759–777 (1997).

9. W. N. Patten, C. Mo, J. Kuehn and J. Lee, 'A primer on design of semiactive vibration absorbers (SAVA)', *J. Engng. Mech. ASCE* **124**(1), 61–68 (1998).
10. W. N. Patten, 'The I-35 Walnet Creek Bridge: an intelligent highway bridge via semi-active structural control', *Proc. 2nd World Conf. on Structural Control*, 1998, Vol. 1, pp. 427–436.
11. Z. Akbay and H. M. Aklan, 'Intelligent energy dissipation devices', *Proc. 4th U.S. Nat. Conf. on Earthquake Engineering*, 1990, Vol. 3, pp. 427–435.
12. D. J. Dowdell and S. Cherry, 'Structural control using semi-active friction dampers', *Proc. 1st World Conf. on Structural Control*, 1994, Vol. 1, FA1, pp. 59–68.
13. Q. Feng, M. Shinozuka and S. Fujii, 'Friction-controllable sliding isolated systems', *J. Engng. Mech. ASCE* **119**(9), 1845–1864 (1993).
14. J. N. Yang, J. C. Wu and S. Y. Hsu, 'Parametric control of seismic-excited structures', *Proc. 1st World Conf. on Structural Control*, 1994, Vol. 1, WP1, pp. 88–97.
15. J. Hirai, M. Naruse and H. Abiru, 'Structural control with variable friction damper for seismic response', *Proc. 11th World Conf. on Earthquake Engineering*, Paper No. 1934, 1996.
16. R. C. Ehrgott and S. F. Masri, 'Structural control applications of an electrorheological device', *Proc. Int. Workshop on Structural Control*, 1993, pp. 115–129.
17. H. P. Gavin, R. D. Hanson and N. H. McClamroch, 'Control of structures using electrorheological dampers', *Proc. 11th World Conf. on Earthquake Engineering*, Paper No. 272, 1996.
18. N. Makris, D. Hills, S. Burton and M. Jordan, 'Electrorheological fluid dampers for seismic protection of structures', *Proc. SPIE Conf. on Smart Struct. and Mater*, *I*, 1995, pp. 184–194.
19. B. F. Spencer Jr., S. J. Dyke and M. K. Sain, 'Magnetorheological dampers: a new approach to seismic protection of structures', *Proc. Conf. on Decision and Control*, 1996, pp. 676–681.
20. J. D. Carlson and B. F. Spencer Jr., 'Magneto-rheological fluid dampers for semi-active seismic control', *Proc. 3rd Int. Conf. on Motion and Vibrational Control*, 1996, Vol. 3, pp. 35–40.
21. M. Takemura and T. Ikeura, 'A semi-empirical method using a hybrid of stochastic and deterministic fault models: simulation of strong ground motions during large earthquakes', *J. Phys. Earth* **36**, 89–106 (1988).
22. K. Kudo, 'A study on the contribution of surface waves to strong ground motions', *Proc. 7th WCEE*, Istanbul, 1980, Vol. 2, pp. 499–506.

